

A General and Ultrafast Polishing Method with Truly Atomic Roughness

Yi Zhang,[§] Yongjie Zhang,[§] Kaixuan Gu, Linfeng Zhang, Yuanmin Zhu, Dianzi Liu, and Hui Deng*



Cite This: *J. Phys. Chem. Lett.* 2023, 14, 9441–9447



Read Online

ACCESS |



Metrics & More

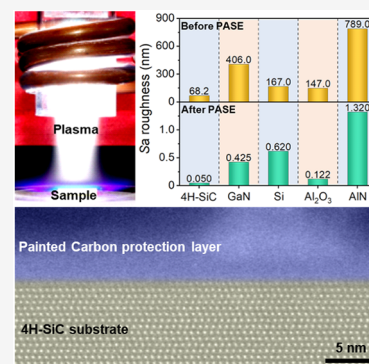


Article Recommendations



Supporting Information

ABSTRACT: The advancement of science and technology is always accompanied by better manufacturing precision. Ideally, the highest precision for manufacturing a surface is truly atomic flatness, which implies that all topmost surface atoms are in a single layer of the crystal face. However, almost no methods can achieve this surface with high efficiency at present. Herein, we present a method to fabricate a large-scale truly atomically flat surface with ultrafast speed. Through the selective etching of surface atoms, our method can achieve an atomically flat surface with 0.05 nm Sa roughness. It is notable that the polishing efficiency of our method is more than 1000 times higher than that of conventional methods. We have demonstrated its generality on various single-crystal materials and obtained atomic roughness and an ultrahigh polishing rate. This method has the potential to promote the mass-production of atomic-scale smooth surfaces, the application of third-generation semiconductor materials, and the innovation of advanced technologies.



The advancement of manufacturing technologies is the foundation for the development of human civilization. From the craft-based manufacturing originated over 4000 B.C. to the automatic production using machinery developed since the second industrial revolution, manufacturing precision has evolved from millimeter to micrometer and nanometer.¹ The development of manufacturing technologies has always been chasing higher precision. Fang et al. conclude the next phase of manufacturing is atomic and close-to-atomic scale manufacturing (ACSM), where material removal, transformation, and addition are at atomic precision.² One of the important fields of ACSM is the manufacturing of an atomic-level surface, which means ideally all atoms within the surface are in the same layer of the crystal plane. This is also known as the roughness limit of a surface in the field of applied physics.³ Many state-of-the-art methods have been invented and developed to approach this goal. However, due to machine tools' precision, volumetric removal with large amount of atoms, and low atomic manipulation efficiency, fabricating a large-scale surface with true-atomic-level precision is still challenging.²

Substantial effort has been devoted to obtaining an ultrasurface with subnanometer roughness. Here we divided them into three categories: polishing method, exfoliation method, and tip-based method. The polishing method, which can fabricate a relatively large-scale surface, can be categorized into mechanical methods and hybrid-mechanical methods. A mechanical method such as nanogrinding can avoid brittle fracture, as it can precisely control the grain depth cut to be equal to or less than the critical depth of ductile removal.⁴ To obtain a gentle loading pressure, magneto-

rheological fluid, fluid jet, and bonnet are often used to carry the abrasives.^{5–7} Although this method can suppress micro-cracks and achieve subnanometer roughness, the formation of an amorphous layer and subsurface damage is inevitable due to the nature of ductile deformation.⁸ Hybrid-mechanical methods can modify the sample surface via different mechanisms, which would make the material removal easier. The most commonly used surface modification approach is chemical reaction,⁹ and its derivative methods such as electrochemical¹⁰ and photocatalytic reaction¹¹ are also adopted. However, these methods generally show quite a low efficiency for high-hardness and chemically inert materials. For both mechanical and hybrid-mechanical methods, the ductile mode removal mechanism is eventually employed to understand the removal of surface material. It is impossible to confine the energy of each grain within the need to remove an atom, and the exceeding force will always influence the subsurface atoms. Thus, it is very difficult to achieve atomic precision with mechanical-involved methods. However, methods that are based on chemical etching and have no contact force with surface atoms can overcome this problem.

Exfoliation methods are widely used for the fabrication of emergent 2D materials. The world's first piece of graphene was prepared through mechanical exfoliation, and the investigation

Received: August 19, 2023

Accepted: October 9, 2023

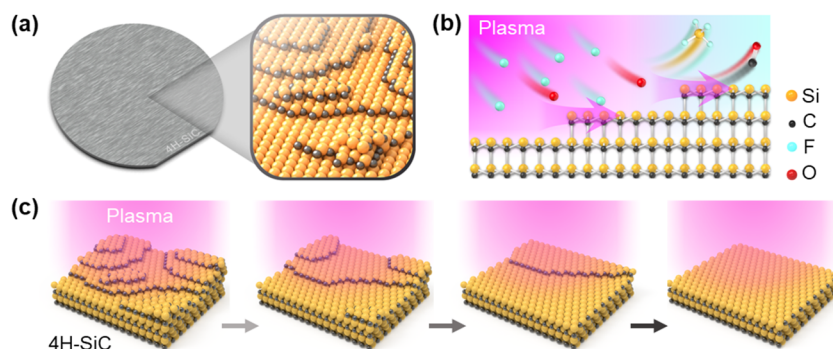


Figure 1. Mechanism of PASE for the polishing of 4H-SiC. (a) Schematic of a sliced 4H-SiC wafer and the atomic surface after magnification (right). (b) Schematic of the PASE process. (c) Schematic of the evolution of surface topography during PASE.

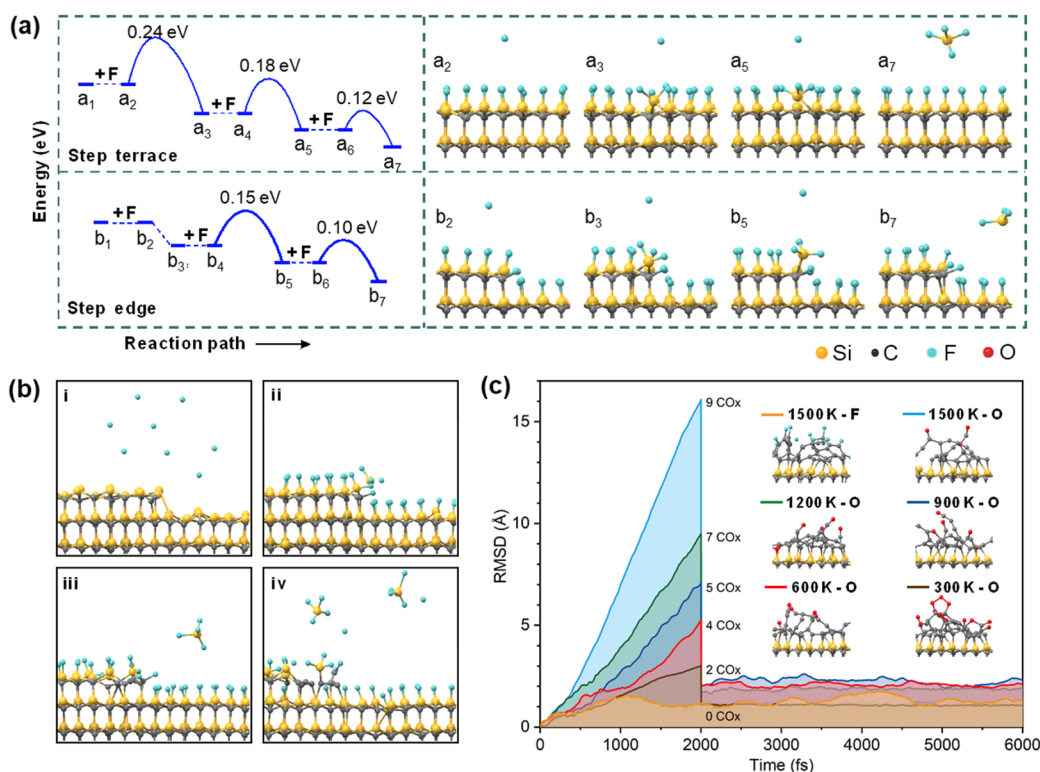


Figure 2. AIMD simulation of the PASE process for 4H-SiC. (a) Reaction paths of ST atom and SE atom. (b) An atomic step etched by F multiple times. (c) Root-mean-square deviation (RMSD) curve of the surface carbon layer etched by the O atoms at 300–1500 K or by the F atoms at 1500 K.

of many intrinsic properties, such as quantum Hall effect and superconductivity, are explored based on graphene obtained by the exfoliation method.^{12–14} More recently, ion-intercalation, liquid exfoliation, electrochemically assisted exfoliation, and Au-assisted exfoliation have greatly improved the usability of this method.^{15–18} However, the exfoliation method is only applicable for 2D materials, and it is still limited in lateral size, yield, and unexpected contaminations.

The most controllable method which can achieve true atomic precision is a tip-based method. Using scanning tunneling microscopy (STM) or atomic force microscopy (AFM), researchers can accurately manipulate a single atom.^{19,20} The removal of a single atomic layer within a relatively large area of micrometer level has also been achieved by an AFM-based mechanochemical reaction.²¹ However, it is difficult to exceed one micrometer scale by tip-based methods, which is still too small for device applications. Because of the

ultralow efficiency, high demand for expensive vacuum equipment, and the need for highly skilled operators, applications of the tip-based method are limited.

To fabricate a large-scale and true atomically flat surface, advance the limitation of polishing technology, and facilitate the application of difficult-to-machine materials, we propose the plasma-based atom-selective etching (PASE) method. PASE is based on the selective removal of surface atoms which constitute the surface roughness, and this is also the most direct way to reduce roughness without influencing the subsurface material.^{22,23} As shown in Figure 1a, the rough surface of single-crystal silicon carbide (4H-SiC) is formed by many atomic steps. The chemical activity of the atom on the step edge (SE atom) and the step terrace (ST atom) is different.^{24,25} Under the appropriate conditions (herein, we adopt plasma etching), the etching speed of SE atoms can be much larger than that of ST atoms, and thus, etching can

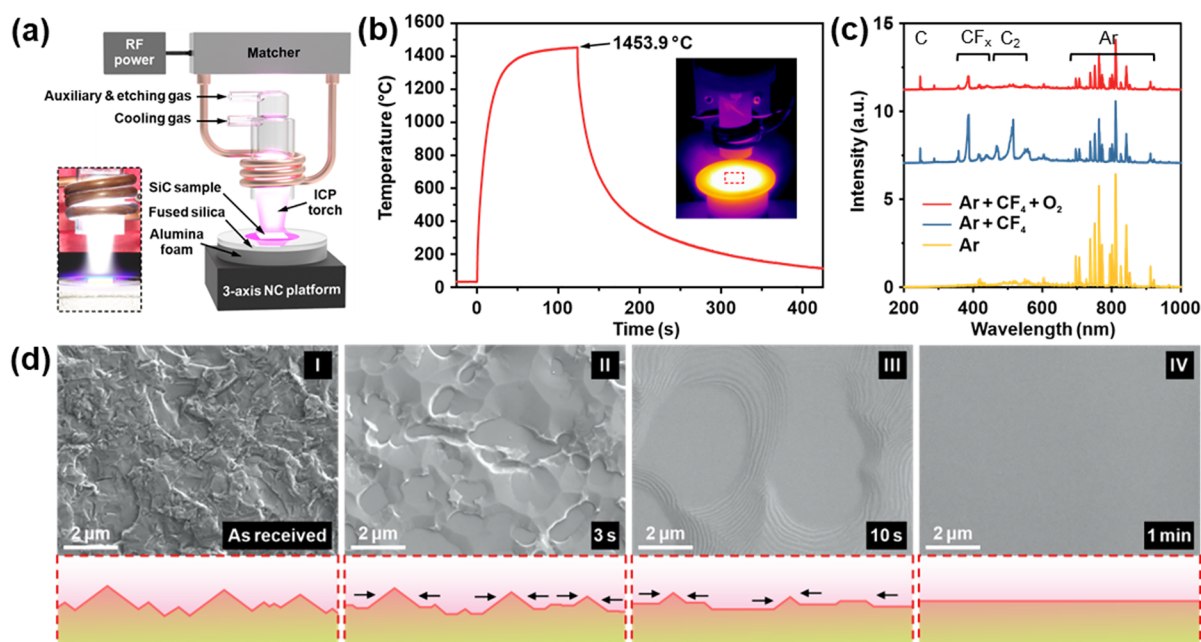


Figure 3. Experimental setup and PASE results of 4H-SiC. (a) Schematic diagram of experimental setup. (b) Sample surface temperature during PASE, where the whole operation time is 120 s. (c) OES results of the ICP torch with different reaction gases. (d) Scanning electron microscopy (SEM) images of the sample surface and the corresponding schematic of the sample cross section during PASE.

extend along the step edge, as shown in Figure 1b. When atom-selective etching is applied on all the SE atoms on the surface, the atomic step edge can be quickly removed. As shown in Figure 1c and Movie S1, the atoms constituting surface roughness could be removed, and eventually, a true-atomically flat surface is formed. The selective lateral etching can remove the unwanted atomic layers until all atoms achieve an equipotential state, which means all atoms are ideally located forming an integral crystal plane with truly atomic flatness. Therefore, PASE can be regarded as a polishing technology that can achieve the ultimate surface roughness.

In addition to its most important feature of obtaining an atomic-level surface, PASE also has the characteristics of ultrahigh efficiency and universal applicability to crystalline materials. As an etching process using atmospheric high-temperature and high-particle-density plasma, PASE shows ultrafast polishing efficiency, compared with conventional polishing, exfoliation, and tip-based manipulation approaches. Unlike other existing precision surface manufacturing methods which could only start with raw surface with nano- or subnanometer roughness, this work would only take 5 min to directly polish a sliced 4H-SiC chip with Sa roughness on the order of hundreds of nanometers to the atomically smooth state with 0.05 nm Sa roughness. To achieve the atomic-scale smooth 4H-SiC surface, conventional chemical mechanical polishing (CMP) generally needs more than 8 h, as shown in Figure S1. Compared with the exfoliation method and tip-based method, which can only generate atomic surfaces within a micrometer level area, PASE is able to produce centimeter level atomic surface.

For the surface of any crystalline material, unless it achieves a surface where surface atoms are regularly arranged with the same potential energy, there will be differences in the etching of atoms at different sites on the surface. Thus, PASE has the potential to be applied as a general polishing method for single-crystal materials. In this work, we have demonstrated the atomic scale polishing of 4H-SiC, GaN, Si, Al₂O₃, and AlN.

PASE can greatly increase the polishing efficiency of many difficult-to-machine single-crystal materials and facilitate the application of next-generation semiconductor materials. PASE could be easily applied on large-size samples if a broad-scale and even plasma environment could be produced.

As a typical next-generation semiconductor and hard-to-machine material, 4H-SiC has been chosen to demonstrate the advancement of the PASE method. We first adopted ab initio molecular dynamics (AIMD) simulation to analyze the etching process and explore the appropriate condition for the selective etching of surface atoms. As shown in Figures 2a and S2, the dissociate paths of step-edge Si atom (SE-Si) and step-terrace Si atom (ST-Si) under the irradiation of fluorine plasma are different. The calculated activation energies for SE-Si and ST-Si under 300 K are 0.25 and 0.54 eV respectively. According to the Arrhenius equation, the etching of SE-Si should be 74435 times higher than that of ST-Si.²⁶ However, fluorine plasma never shows such great lateral etching ability under room temperature in an actual etching operation. We further extended the etching time to capture more details about PASE, as shown in Figures 2b and S3. After a few cycles of selective etching of SE-Si, we observed accumulation of amorphous carbon remaining on the surface. Those amorphous carbons would hinder step edges and thus would be an obstacle for the following selectivity toward SE-Si. Thus, we introduced oxygen into the plasma to remove the amorphous carbon. As shown in Figure 2c, the ability to remove absorbed carbon is weak under low temperature while higher temperature dramatically strengthens this ability.²⁷ Meanwhile, the absorption of O atoms on the 4H-SiC surface can produce relatively loose Si–O structure, forming active sites that are easy to be etched. The amount of generated CO_x increases rapidly with the increase of temperature. Additionally, under 1500 K, carbon has not dissociated with the same amount of injecting F atoms, implying that O has much higher carbon removal ability than F. In summary, the combination of F and O plasmas can be used to realize atom-selective etching

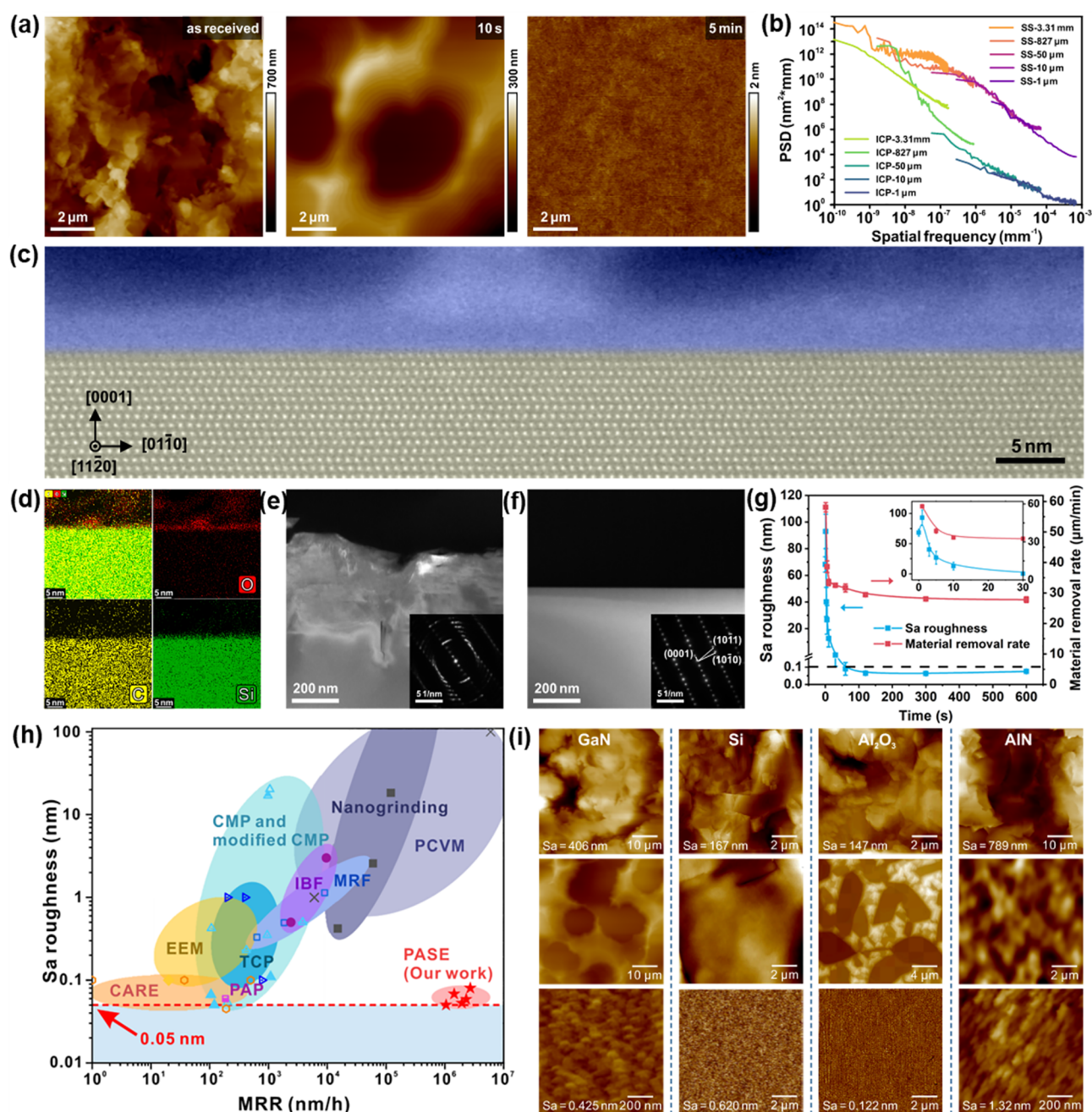


Figure 4. Ultrafast and atomic roughness polishing by PASE. (a) AFM images of 4H-SiC samples with different plasma durations. (b) PSD curves of 4H-SiC samples before and after PASE. (c) STEM image of the cross section of the 4H-SiC sample after PASE. (d) Element mapping results. (e and f) STEM images and SAED patterns of (e) as-received 4H-SiC sample and (f) polished 4H-SiC sample via PASE. (g) The roughness and MRR variations of 4H-SiC during PASE. (h) The comparison between PASE and other cutting-edge polishing methods. (i) AFM images of various single-crystal materials polished by PASE.

of 4H-SiC. F atoms serve as the main element to the selective etching of SE-Si, and the etching speed is calculated to be 74435 times higher than that of ST-Si. O atoms can remove the accumulated amorphous carbon and expose the Si atoms behind. The carbon removal ability of O increases rapidly with temperature. Significantly, O would form a loose Si–O structure on the surface, which can accelerate the etching process. At the macro level, the synergy of F and O could be an effective path for highly efficient etching of atomic steps on 4H-SiC. Therefore, the key point to achieve atom-selective etching of 4H-SiC is to modulate F and O atoms to an appropriate ratio and impose high temperature.

According to the simulation results, a dense and high-temperature plasma that contains an appropriate proportion of F and O radicals is required for the PASE process. Herein, we utilize atmospheric pressure inductively coupled plasma (ICP) as the etchant to experimentally demonstrate the atomic-scale polishing ability of PASE. An ICP torch can provide both high-temperature and high-radical-density plasma.²⁸ Meanwhile, as our plasma works under atmospheric pressure, which implies a low mean-free path, it would not introduce new damage caused by atomic bombardment commonly observed in low-pressure and vacuum plasma.²⁹ The schematic experimental setup is shown in Figure 3a. The sample stage was made from

alumina foam to maintain the high temperature of the sample surface during PASE. A piece of quartz glass was placed on the foam to prevent powder contamination. During a typical polishing process, the ICP was ignited outside the substrate and then moved to a predefined location. The temperature of the sample would quickly rise to over 1400 °C in 60 s (Figure 3b), and the heating rate is much higher than conventional furnaces or heating tables. The temperature can be regulated by modulating the radio frequency (RF) power and stand-off distance (Figure S4). After the PASE process was conducted for the set duration, the RF power would be turned off and the 4H-SiC sample was cooled under the protection of Ar flow. Figure 3c shows the optical emission spectroscopy (OES) of ICP. After the addition of CF₄ into the plasma, a strong CF_x (350–450 nm) peak and typical C₂ (450–570 nm) Swan system can be observed clearly.^{30–32} However, a high concentration of C₂ could increase the surface absorption of carbon, which can hide the atomic step structure and impede the preferential edge etching effect. When oxygen is added, the intensity of the C₂ peak greatly decreased. Oxygen is also a highly electronegative gas, which can gain energy from energetic electrons and compete with CF₄; thus, it can be seen that the intensity of the CF_x peak is also reduced.³³ The peak at 777.6 nm represents the transitions of O atoms (3p5P → 3s5S), suggesting that abundant O radicals could be used to remove the accumulated carbon layer.³⁴ The radical percentage can be controlled by modifying the input flow rates of CF₄ and O₂ (Figure S5). Therefore, this plasma source is considered to be able to meet the requirements for the realization of PASE.

The surface morphology of the etched 4H-SiC sample and the corresponding schematic diagram of surface profiles are shown in Figure 3d. The as-received surface of 4H-SiC, which is rough and seriously damaged, is preprocessed by slicing. Within 3 s, the amorphous layer on the surface has been quickly removed, as amorphous 4H-SiC contains more dangling bonds which should be easy to be etched. The surface processed by 3 s of etching already shows some small flat bottoms, which implies the significant role of lateral etching effect. After 10 s of PASE, the surface demonstrates even more pronounced iconic flat bottoms, further confirming the lateral etching effect. With the etching going on, the flat bottom continually expanded and finally combined together, forming an integral flat surface without any steps and terraces, which could be observed on the sample surface processed by PASE for 1 min. The schematic diagram in Figure 3d and Movie S2 graphically show how the lateral etching can result in flat bottoms and eventually form an ultrasmooth surface. This set of samples can clearly prove that PASE can achieve a lateral etching effect and polish the sample efficiently.

The selective etching effect in PASE was further confirmed by AFM. As shown in Figure 4a, within 10 s, selective etching sites with a flat bottom are formed on a rough sliced surface. In 5 min, all atom steps disappear and the Sa roughness decreases to 0.05 nm. The power spectral density (PSD) curves in Figure 4b show an improvement of all spatial frequencies, and meanwhile, it takes only 5 min to converge to the final PSD shown in Figure S6. The scanning transmission electron microscopy (STEM) result in Figure 4c shows the cross-sectional profile of the surface etched for 5 min, and a carbon layer was used to protect the topmost layer of atoms in the focused ion beam (FIB) process.³⁵ It can be seen clearly that the surface layer is an integrated crystal plane surface without defects, missing atoms, and extra atoms. The energy dispersive

spectrometry (EDS) result in Figure 4d shows that only protective carbon paint layer (containing carbon and oxide) remains on the surface. To ensure that all the amorphous layers are from protective painting rather than the PASE polishing process, we have also prepared an FIB sample protected by electron beam evaporated Cr layer, and the result also indicates that the surface was well-crystallized and atomically flat 4H-SiC (Figure S7). We obtained the lower-magnification STEM images of 4H-SiC before and after PASE, and the results are shown in Figure 4e,f. The raw surface is heavily damaged, and many strain patterns can be observed. The heavily twisted selected area electron diffraction (SAED) pattern also confirms the finding.³⁶ After PASE, the polished surface is visually uniform, and the typical SAED pattern of 11 $\bar{2}$ 0 zone-axis implies the good crystallinity of the surface region,³¹ suggesting that the subsurface damage (SSD) layer has been removed.

The PASE process is based on the selective etching of SE atoms, which can also be interpreted as a much higher lateral etching speed compared with the vertical direction. This means the material removal rate (MRR) should be closely related to the surface roughness, as a higher roughness implies more exposed atomic step edges. The roughness and MRR are shown in Figure 4g. During the first minute of etching, the roughness rapidly decreased from 68.2 to 0.1 nm, then slowly reduced to 0.05 nm in 5 min, and finally remained at that roughness. The MRR also decreased from 58.1 to 31.7 $\mu\text{m}/\text{min}$ in the first minute of PASE and then converted to around 30 $\mu\text{m}/\text{min}$, which also proved the atom-selective etching mechanism. We compared PASE with many conventional and cut-edge methods, as shown in Figure 4h and Table S1. It can be found that PASE can reach the lowest roughness, while its efficiency is 3 orders of magnitude higher than that of the other methods. Meanwhile, PASE is theoretically able to reach truly atomic flatness, while other methods are not capable of that achievement. The PASE method breaks the rule that high MRR will result in a rough surface; when MRR increases in PASE, the roughness remains almost the same with atomic level (Figure S8).

We further demonstrated the general ability of PASE. Theoretically, all single-crystal materials could be polished by PASE. Herein, we explore the polishing of several typical difficult-to-machine materials, including GaN, Si, Al₂O₃, and AlN, via PASE, and the results are shown in Figure 4i. It is clear that all these materials have reached atomic flatness from the sliced raw surface in several minutes. Meanwhile, the localized flat bottom morphology emerged in all samples during etching. These results suggest that PASE is practical in polishing a wide range of single crystals. These results strongly demonstrate that PASE has the potential to be industrially utilized for the manufacturing of single-crystal wafers with truly atomic flatness and ultrahigh efficiency with a level of $\mu\text{m}/\text{min}$.

PASE can produce a true atomically flat surface of single-crystal materials with ultrahigh efficiency. By controlling the plasma scale, uniformity, and temperature, it can be readily extended to process large size wafers.³⁷ PASE has the ability to substitute the lapping, mechanical polishing, and chemical mechanical polishing steps in conventional wafer manufacturing processes and greatly reduce the time cost. For instance, in this work, the polishing process of 4H-SiC has been reduced from over 8 h to less than 10 min, which could reduce 12% of the manufacturing cost.³⁸ Thus, PASE will foster the application of devices based on them. The PASE process can

be coupled with a subsequent deposition or oxidation process, since the high-temperature and gas-phase environment needed for them are similar. Meanwhile, the ability of PASE to produce true atomically flat surfaces will enable many cutting-edge applications that are possible with truly atomic surfaces, such as quantum chips, single-molecule electronics, and so forth.^{39,40}

■ ASSOCIATED CONTENT

SI Supporting Information

The Supporting Information is available free of charge at <https://pubs.acs.org/doi/10.1021/acs.jpcllett.3c02322>.

Materials and Method; Time consuming comparison, free energy surfaces, AIMD simulations, temperature variations, OES results, PSD results, STEM images, and MRR and Sa roughness results of PASE for 4H-SiC (Figures S1–S8); Comparison of ultra precision polishing methods (Table S1) (PDF)

Movie S1: evolution of surface topography during PASE (MP4)

Movie S2: schematic of the sample cross section during PASE (MP4)

■ AUTHOR INFORMATION

Corresponding Author

Hui Deng – Department of Mechanical and Energy Engineering, Southern University of Science and Technology, Shenzhen 518055 Guangdong, China; orcid.org/0000-0002-7116-7188; Email: dengh@sustech.edu.cn

Authors

Yi Zhang – Department of Mechanical and Energy Engineering, Southern University of Science and Technology, Shenzhen 518055 Guangdong, China; School of Engineering, Faculty of Science, University of East Anglia, Norwich NR4 7TJ, United Kingdom

Yongjie Zhang – Department of Mechanical and Energy Engineering, Southern University of Science and Technology, Shenzhen 518055 Guangdong, China; Department of Physics and Centre for Advanced 2D Materials, National University of Singapore, Singapore 117551, Singapore

Kaixuan Gu – Department of Mechanical and Energy Engineering, Southern University of Science and Technology, Shenzhen 518055 Guangdong, China

Linfeng Zhang – Department of Mechanical and Energy Engineering, Southern University of Science and Technology, Shenzhen 518055 Guangdong, China

Yuanmin Zhu – Department of Materials Science and Engineering and Academy for Advanced Interdisciplinary Studies, Southern University of Science and Technology, Shenzhen 518055 Guangdong, China

Dianzi Liu – School of Engineering, Faculty of Science, University of East Anglia, Norwich NR4 7TJ, United Kingdom

Complete contact information is available at:

<https://pubs.acs.org/doi/10.1021/acs.jpcllett.3c02322>

Author Contributions

[§]Yi Zhang and Yongjie Zhang contributed equally to this work. Hui Deng supervised the project. Yi Zhang performed the experiment and characterization. Yongjie Zhang and Kaixuan Gu contributed to the AIMD calculations and the mechanism

analysis of PASE. Linfeng Zhang and Yuanmin Zhu contributed to the TEM characterization. Dianzi Liu contributed to useful discussions. All the authors contributed to the writing of the manuscript. Hui Deng and Yongjie Zhang revised the manuscript.

Notes

The authors declare no competing financial interest.

■ ACKNOWLEDGMENTS

This project is supported by the National Natural Science Foundation of China (52005243) and the Science and Technology Innovation Committee of Shenzhen Municipality (JCYJ20220818100412027, JCYJ20210324120402007). The authors acknowledge the assistance of SUSTech Core Research Facilities.

■ REFERENCES

- (1) Kalpakjian, S.; Schmid, S. R. *Manufacturing Engineering and Technology*; Pearson, 2001.
- (2) Fang, F.; Zhang, N.; Guo, D.; Ehmann, K.; Cheung, B.; Liu, K.; Yamamura, K. Towards Atomic and Close-to-Atomic Scale Manufacturing. *Int. J. Extreme Manuf.* **2019**, *1*, 012001.
- (3) Yu, J.; Namba, Y. Atomic Surface Roughness. *Appl. Phys. Lett.* **1998**, *73*, 3607–3609.
- (4) Yin, L.; Pickering, J. P.; Ramesh, K.; Huang, H.; Spowage, A. C.; Vancoille, E. Y. J. Planar Nanogrinding of a Fine Grained WC-Co Composite for an Optical Surface Finish. *Int. J. Adv. Manuf. Technol.* **2005**, *26*, 766–773.
- (5) Kordonski, W. I.; Jacobs, S. D. Magnetorheological Finishing. *Int. J. Mod. Phys. B* **1996**, *10*, 2837–2848.
- (6) Walker, D. D.; Brooks, D.; Freeman, R.; King, A.; McCavana, G.; Morton, R.; Riley, D.; Simms, J. First Aspheric Form and Texture Results from a Production Machine Embodying the Precession Process. In *International Symposium on Optical Science and Technology*; Stahl, H. P., Ed.; Society of Photo-Optical Instrumentation Engineers: San Diego, CA, 2001; Vol. 4451, pp 267–276.
- (7) Booiij, S. M. Nanometer Deep Shaping with Fluid Jet Polishing. *Opt. Eng.* **2002**, *41*, 1926–1931.
- (8) Ngoi, B. K. A.; Sreejith, P. S. Ductile Regime Finish Machining - A Review. *Int. J. Adv. Manuf. Technol.* **2000**, *16*, 547–550.
- (9) Aida, H.; Doi, T.; Takeda, H.; Katakura, H.; Kim, S.-W.; Koyama, K.; Yamazaki, T.; Uneda, M. Ultraprecision CMP for Sapphire, GaN, and SiC for Advanced Optoelectronics Materials. *Curr. Appl. Phys.* **2012**, *12*, S41–S46.
- (10) Murata, J.; Yodogawa, K.; Ban, K. Polishing-Pad-Free Electrochemical Mechanical Polishing of Single-Crystalline SiC Surfaces Using Polyurethane-CeO₂ Core-Shell Particles. *Int. J. Mach. Tools Manuf.* **2017**, *114*, 1–7.
- (11) Wang, W.; Zhang, B.; Shi, Y.; Zhou, J.; Wang, R.; Zeng, N. Improved Chemical Mechanical Polishing Performance in 4H-SiC Substrate by Combining Novel Mixed Abrasive Slurry and Photocatalytic Effect. *Appl. Surf. Sci.* **2022**, *575*, 151676.
- (12) Novoselov, K. S.; Geim, A. K.; Morozov, S. V.; Jiang, D.; Zhang, Y.; Dubonos, S. V.; Grigorieva, I. V.; Firsov, A. A. Electric Field Effect in Atomically Thin Carbon Films. *Science* **2004**, *306*, 666–669.
- (13) Zhang, Y.; Tan, Y. W.; Stormer, H. L.; Kim, P. Experimental Observation of the Quantum Hall Effect and Berry's Phase in Graphene. *Nature* **2005**, *438*, 201–204.
- (14) Cao, Y.; Fatemi, V.; Fang, S.; Watanabe, K.; Taniguchi, T.; Kaxiras, E.; Jarillo-Herrero, P. Unconventional Superconductivity in Magic-Angle Graphene Superlattices. *Nature* **2018**, *556*, 43–50.
- (15) Coleman, J. N.; Lotya, M.; O'Neill, A.; Bergin, S. D.; King, P. J.; Khan, U.; Young, K.; Gaucher, A.; De, S.; Smith, R. J.; et al. Two-Dimensional Nanosheets Produced by Liquid Exfoliation of Layered Materials. *Science* **2011**, *331*, 568–571.

- (16) Fan, X.; Xu, P.; Zhou, D.; Sun, Y.; Li, Y. C.; Nguyen, M. A.; Terrones, M.; Mallouk, T. E. Fast and Efficient Preparation of Exfoliated 2H MoS₂ Nanosheets by Sonication-Assisted Lithium Intercalation and Infrared Laser-Induced 1T to 2H Phase Reversion. *Nano Lett.* **2015**, *15*, 5956–5960.
- (17) Ambrosi, A.; Pumera, M. Exfoliation of Layered Materials Using Electrochemistry. *Chem. Soc. Rev.* **2018**, *47*, 7213–7224.
- (18) Huang, Y.; Pan, Y. H.; Yang, R.; Bao, L. H.; Meng, L.; Luo, H. L.; Cai, Y. Q.; Liu, G. D.; Zhao, W. J.; Zhou, Z.; et al. Universal Mechanical Exfoliation of Large-Area 2D Crystals. *Nat. Commun.* **2020**, *11*, 2453.
- (19) Hla, S. W. Atom-by-Atom Assembly. *Rep. Prog. Phys.* **2014**, *77*, 056502.
- (20) Custance, O.; Perez, R.; Morita, S. Atomic Force Microscopy as a Tool for Atom Manipulation. *Nat. Nanotechnol.* **2009**, *4*, 803–810.
- (21) Chen, L.; Wen, J.; Zhang, P.; Yu, B.; Chen, C.; Ma, T.; Lu, X.; Kim, S. H.; Qian, L. Nanomanufacturing of Silicon Surface with a Single Atomic Layer Precision via Mechanochemical Reactions. *Nat. Commun.* **2018**, *9*, 1542.
- (22) Fang, Z.; Zhang, Y.; Li, R.; Liang, Y.; Deng, H. An Efficient Approach for Atomic-Scale Polishing of Single-Crystal Silicon via Plasma-Based Atom-Selective Etching. *Int. J. Mach. Tools Manuf.* **2020**, *159*, 103649.
- (23) Deng, H.; Zhang, Y.; Liang, J.; Zhang, X. Surface Reconstruction of Sapphire at the Atomic Scale via Chemical-Physical Tuning of Atmospheric Plasma. *CIRP Ann. Manuf. Technol.* **2023**, *72*, 489–492.
- (24) Shen, A.; Zou, Y.; Wang, Q.; Dryfe, R. A.; Huang, X.; Dou, S.; Dai, L.; Wang, S. Oxygen Reduction Reaction in a Droplet on Graphite: Direct Evidence That the Edge Is More Active Than the Basal Plane. *Angew. Chem., Int. Ed. Engl.* **2014**, *53*, 10804–10808.
- (25) Shao, M.; Peles, A.; Shoemaker, K. Electrocatalysis on Platinum Nanoparticles: Particle Size Effect on Oxygen Reduction Reaction Activity. *Nano Lett.* **2011**, *11*, 3714–3719.
- (26) Laidler, K. J. The Development of the Arrhenius Equation. *J. Chem. Educ.* **1984**, *61*, 494–498.
- (27) Li, C. E.; Brown, T. C. Carbon Oxidation Kinetics from Evolved Carbon Oxide Analysis During Temperature-Programmed Oxidation. *Carbon* **2001**, *39*, 725–732.
- (28) Tendero, C.; Tixier, C.; Tristant, P.; Desmaison, J.; Leprince, P. Atmospheric Pressure Plasmas: A Review. *Spectrochim Acta B* **2006**, *61*, 2–30.
- (29) Bárdos, L.; Baránková, H. Plasma Processes at Atmospheric and Low Pressures. *Vacuum* **2008**, *83*, 522–527.
- (30) Wang, R.; Zhang, C.; Liu, X.; Xie, Q.; Yan, P.; Shao, T. Microsecond Pulse Driven Ar/CF₄ Plasma Jet for Polymethylmethacrylate Surface Modification at Atmospheric Pressure. *Appl. Surf. Sci.* **2015**, *328*, 509–515.
- (31) Zhang, Y.; Zhang, L.; Chen, K.; Liu, D.; Lu, D.; Deng, H. Rapid Subsurface Damage Detection of SiC Using Inductively Coupled Plasma. *Int. J. Extreme Manuf.* **2021**, *3*, 035202.
- (32) Resnik, M.; Zaplotnik, R.; Mozetic, M.; Vesel, A. Comparison of SF₆ and CF₄ Plasma Treatment for Surface Hydrophobization of PET Polymer. *Mater.* **2018**, *11*, 311.
- (33) Kimura, T.; Noto, M. Experimental Study and Global Model of Inductively Coupled CF₄/O₂ Discharges. *J. Appl. Phys.* **2006**, *100*, 063303.
- (34) Zhou, R.-W.; Zhang, X.-H.; Zong, Z.-C.; Li, J.-X.; Yang, Z.-B.; Liu, D.-P.; Yang, S.-Z. Reactive Oxygen Species in Plasma Against *E. Coli* Cells Survival Rate. *Chin. Phys. B* **2015**, *24*, 085201.
- (35) Schaffer, M.; Schaffer, B.; Ramasse, Q. Sample Preparation for Atomic-Resolution STEM at Low Voltages by FIB. *Ultramicroscopy* **2012**, *114*, 62–71.
- (36) Yan, J.; Gai, X.; Harada, H. Subsurface Damage of Single Crystalline Silicon Carbide in Nanoindentation Tests. *J. Nanosci. Nanotechnol.* **2010**, *10*, 7808–7811.
- (37) Lee, K.; Lee, Y.; Jo, S.; Chung, C.-W.; Godyak, V. Characterization of a Side-Type Ferrite Inductively Coupled Plasma Source for Large-Scale Processing. *Plasma Sources Sci. Technol.* **2008**, *17*, 015014.
- (38) Reese, S. B.; Singh, A.; Zakutayev, A.; Akar, S.; Remo, T. Why Wideband Gap Needs Techno-Economics. In *2019 IEEE 7th Workshop on Wide Bandgap Power Devices and Applications (WIPDA)*; IEEE, 29–31 October, **2019**; Raleigh, NC; pp 337–341.
- (39) Joachim, C.; Martrou, D.; Rezeq, M.; Troadec, C.; Jie, D.; Chandrasekhar, N.; Gauthier, S. Multiple Atomic Scale Solid Surface Interconnects for Atom Circuits and Molecule Logic Gates. *J. Condens. Matter Phys.* **2010**, *22*, 084025.
- (40) Wu, L.; Wang, A.; Shi, J.; Yan, J.; Zhou, Z.; Bian, C.; Ma, J.; Ma, R.; Liu, H.; Chen, J.; et al. Atomically Sharp Interface Enabled Ultrahigh-Speed Non-Volatile Memory Devices. *Nat. Nanotechnol.* **2021**, *16*, 882–887.